



HAL
open science

Defects in 15-HETE Production and Control of Epithelial Permeability by Human Enteric Glial Cells From Patients With Crohn's Disease

Camille Pochard, Sabrina Coquenlorge, Julie Jaulin, Nicolas Cenac, Nathalie Vergnolle, Guillaume Meurette, Marie Freyssinet, Michel Neunlist, Malvyne Rolli-Derkinderen

► **To cite this version:**

Camille Pochard, Sabrina Coquenlorge, Julie Jaulin, Nicolas Cenac, Nathalie Vergnolle, et al.. Defects in 15-HETE Production and Control of Epithelial Permeability by Human Enteric Glial Cells From Patients With Crohn's Disease. *Gastroenterology*, 2016, 150 (1), pp.168-180. 10.1053/j.gastro.2015.09.038 . hal-03153620

HAL Id: hal-03153620

<https://cnrs.hal.science/hal-03153620>

Submitted on 3 Mar 2021

HAL is a multi-disciplinary open access archive for the deposit and dissemination of scientific research documents, whether they are published or not. The documents may come from teaching and research institutions in France or abroad, or from public or private research centers.

L'archive ouverte pluridisciplinaire **HAL**, est destinée au dépôt et à la diffusion de documents scientifiques de niveau recherche, publiés ou non, émanant des établissements d'enseignement et de recherche français ou étrangers, des laboratoires publics ou privés.

Human enteric glial cells are defective for 15-HETE production and epithelial permeability control in Crohn's disease

Short title: 15-HETE regulates epithelial permeability

Camille Pochard,^{1,2,3,4,*} Sabrina Coquenlorge,^{1,2,3,4,*} Julie Jaulin,^{1,2,3,4} Nicolas Cenac,⁵ Nathalie Vergnolle,⁵ Guillaume Meurette,^{1,2,3,4} Marie Freyssinet,^{1,3,4} Michel Neunlist^{1,2,3,4} and Malvyne Rolli-Derkinderen.^{1,2,3,4}

¹ INSERM, UMR913, Nantes, F-44093, France.

² Nantes University, Nantes, F-44093, France.

³ Institut des Maladies de l'Appareil Digestif, IMAD, CHU Nantes, Hopital Hôtel-Dieu, Nantes, F-44093, France.

⁴ Centre de Recherche en Nutrition Humaine, Nantes, F-44093, France.

⁵ INSERM UMR1043, Toulouse, F-33 000, France.

* Authors share co-first authorship

Grant Support This work was funded by the INSERM, Nantes University, the Centre Hospitalier Universitaire (CHU) of Nantes and SanTDige foundation. SC is the recipient of a doctoral fellowship from Inserm-Pays de La Loire. MRD is supported by the Centre National pour la Recherche Scientifique (CNRS). MN is supported by a Contrat d'interface Hospitalier du CHU of Nantes.

Abbreviations AMPK, AMP-activated kinase; CD, Crohn's disease; EGC, enteric glial cells; IEB, intestinal epithelial barrier; IEC, intestinal epithelial cell; JUG, rat enteric glial cell line; PUFA, polyunsaturated fatty acid; ROG, rat enteric glial cells; UC, ulcerative colitis; ZO-1, zonula occludens-1; 15-HETE, 15-hydroxyeicosatetraenoic acid.

Correspondence Malvyne Rolli-Derkinderen or Michel Neunlist, Neuropathies of the enteric nervous system and digestive diseases, INSERM UMR913, School of Medicine, University of Nantes; 1, rue Gaston Veil, NANTES; F-44035, France; Tel: +33 (0)2 40 41 29 74; Fax: +33 (0)2 40 08 75 06; E-mail: malvyne.derkinderen@univ-nantes.fr; Michel.Neunlist@univ-nantes.fr

Disclosures The authors disclose no conflicts.

Transcript Profiling No

Writing Assistance No

Author Contributions MRD and MN designed the research study, supervised the study and wrote the paper. CP, SC, JJ and NC performed experiments. MRD and CP analyzed the data. NC and NV participated in the critical reading of the manuscript. GM managed and provided human surgical samples.

Acknowledgements We are indebted to Tony Durand for quantitative PCR expertise and to Christina Van Itallie (NHLBI, NIH) for providing the MDCK cell lines. Experiments were carried within the small animal exploration facility Cardiex, which is supported by the GIS-IBiSA program.

ABSTRACT

BACKGROUND & AIMS: Enteric glial cells (EGC) produce soluble mediators to regulate intestinal epithelial barrier (IEB) homeostasis. The present study concerns the definition of the EGC polyunsaturated fatty acid (PUFA) metabolite profile and functional studies of EGC and 15-hydroxyeicosatetraenoic acid (15-HETE) on IEB permeability in a physiological or a Crohn's disease (CD) context.

METHODS: The PUFA signatures of rat EGC and 15-HETE dosage on human EGC from control and CD patients were established using high sensitivity liquid chromatography tandem mass spectrometry. A 15-HETE-producing enzyme was identified in rat and human EGC and tissues by immunostaining. The impact of human EGC on IEB permeability was measured in a co-culture model using Caco-2 cells. *In vitro* and *in vivo*, the functional impact of 15-HETE on IEB permeability and on 15-HETE molecular signaling were analyzed using pharmacological approaches and western blot analysis.

RESULTS: EGC expressed 15-lipoxygenase-2 and mostly produced 15-HETE, which increased IEB resistance and decreased IEB permeability. 15-HETE production was reduced in EGC from CD patients compared with those from control patients. CD EGC were also unable to decrease IEB permeability, and 15-HETE addition restored the permeability to control conditions. *In vivo*, inhibition of 15-HETE production increased permeability, thereby reproducing pathological features. 15-HETE regulated IEB permeability through an inhibition of AMP-activated kinase (AMPK) and an increase in *Zonula Occludens-1* expression.

CONCLUSIONS: This study not only presents the first evidence for human EGC functional abnormalities in CD, but also reveals that 15-HETE can control IEB permeability through an AMPK- and ZO-1-dependent pathway.

KEYWORDS: Enteric Nervous System; Inflammatory Bowel Disease; AMPK; ZO-1

INTRODUCTION

Accumulating data demonstrate that under physiological conditions, enteric glial cells (EGC) positively regulate the intestinal epithelial barrier (IEB). Prime evidence for EGC requirement in maintaining IEB homeostasis is the drastic phenotype of mouse models defective for EGC. *In vivo*, severe ablation of EGC induces a fulminant jejunoileitis, characterized by disruption of IEB integrity.^{1, 2} Less severe ablation of EGC increases paracellular permeability in the absence of gut inflammation³ or prior to the development of intestinal inflammation.⁴ Additional arguments are the studies demonstrating that EGC control the major IEB properties of proliferation, differentiation, healing, resistance and permeability.⁵ EGC inhibit intestinal epithelial cell (IEC) proliferation *via* the release of transforming growth factor- β 1⁶ and regulate IEC proliferation and differentiation via the 15-deoxy- $\Delta^{12,14}$ -prostaglandin J₂ (15dPGJ₂).⁷ Both *in vivo* and *in vitro* experiments show that EGC enhance IEB repair following mechanical or inflammatory injury through the production of derived pro-epidermal growth factor.⁸ EGC also increase IEB resistance and reduce paracellular permeability, in part via S-nitrosoglutathione.⁹ EGC have consistently been shown to increase IEB resistance evoked by stressors such as bacteria, inflammatory mediators and skin burn injuries.¹⁰⁻¹² Altogether these studies identify EGC as a source for soluble factors able to reinforce the IEB via paracrine signaling, but no broad glial secretome has been defined, and the production of gliomediators in pathological contexts remains to be determined. This could be of particular interest to understanding pathological mechanisms of inflammatory bowel disease (IBD). Indeed, EGC present abnormalities in Crohn's disease (CD) and ulcerative colitis (UC). First, glial-derived neurotrophic factor expression is significantly higher in the mucosae of patients with UC as compared with those of controls.¹³ In contrast to UC, a reduced number of glial fibrillary acidic protein (GFAP)-positive EGC are present in noninflamed gut specimens of patients with CD.^{2, 13}

However, none of the currently available data provide evidence of EGC dysfunction in IBD that could be responsible for gut dysfunction and/or pathological symptom generation.

Polyunsaturated fatty acid (PUFA) metabolites are bioactive compounds that play an important role in the induction and resolution of inflammation, and characterization of their role in IBD is currently in progress. The major PUFA in the diet is linoleic acid, which is a precursor of arachidonic acid (AA). AA is metabolized via three major biochemical pathways as follows: the cyclooxygenase pathway leading to prostaglandins, prostacyclin and thromboxane; the lipoxygenase (LOX) pathway giving rise to various hydroperoxy and hydroxy (HETE) fatty acids and leukotrienes; the P450-dependent epoxygenase pathway generating epoxyeicosanoids. Previous studies have shown upregulation of COX and LOX in active UC¹⁴ and elevation of thromboxane TXB₂,¹⁵ leukotriene LTB₄¹⁶ and prostaglandin PGE₂¹⁷ in UC and CD. However, their production is attributed to the mucosa¹⁵⁻¹⁷ or more specifically to neutrophils.¹⁸ The contribution of EGC is unknown, but these cells have been reported to produce PGE₂¹⁹ and 15dPGJ₂.⁷

In this study, we wanted to define a part of the EGC secretome, that is the EGC lipidome, by performing PUFA profiling of EGC-conditioned media. In addition, we assessed the functional impact of two PUFA metabolites produced by EGC, and studied the role of 15-hydroxyeicosatetraenoic acid (15-HETE) in the regulation of IEB permeability in the CD pathological context.

Materials and Methods

Human and rat EGC cultures

Cultures of human and adult rat enteric glial cells (EGC) were obtained according to the procedure described by Soret et al.²⁰ Briefly, human EGC originated from noninflamed, macroscopically healthy areas of intestinal resections from control patients (having undergone surgery for colorectal cancer) and those with a diagnosis of CD established according to international criteria. Six control (age, 19–74 y; sex ratio 1:1; 3 colons and 3 ilea) and six CD (Table 1) patients were included in this study.

Sex	Age at surgery	Explant use for EGC culture	Duration of the disease (years)	Treatment at the time of surgery
F	49	colon	24	Anti-TNF- α antibody
F	63	ileum	21	none
M	24	colon	7	none
M	17	ileum	1	Humira
F	28	ileum	11	Imurel + corticoid
F	25	ileum	13	Imurel

Table 1: Main clinical features of patients with Crohn's disease ($n=6$)

Patients gave their informed consent to take part in the study and all procedures were performed according to the guidelines of the French Ethics Committee for Research on Humans and registered under the no. DC-2008-402. Adult rat EGC (ROG) were obtained from entire small intestines of Sprague-Dawley rats. Human EGC and ROG were maintained for 3 to 5 passages in Dulbecco's modified Eagle medium (DMEM, 4.5g/L Glc) supplemented with 10% heat-inactivated fetal calf serum, 2 mmol/L glutamine, 100 IU/mL penicillin and 100 μ g/mL streptomycin. The purity of the cellular population was verified regularly by immunocytochemistry (see Immunocytochemistry). EGC cultures presenting more than 80% GFAP-, Sox10-, and S100 β -positive cells were used for experiments. The rat embryonic cell line (JUG) was obtained as described by Bach-Ngohou et al.⁷ and was studied between passages 18 to 30.

PUFA dosage

The PUFA dosage was performed as described by Le Faouder et al.²¹ and detailed in Suppl Mat 1. The PUFA profile was established in EGC-conditioned media. Five thousand JUG, ROG or HOG were plated in 12-well plates and after 1 day placed in 2 mL defined DMEM medium supplemented with 100 IU/mL penicillin and 100 μ g/mL streptomycin, without any serum. After 3 days,

conditioned media were centrifuged at 14,000 rpm for 5 min at 4°C, 1 mL was used for analysis of permeability and TEER on Caco-2 filters, and 500 µL frozen at -80°C until analysis.

Intestinal epithelial cell (IEC) culture

The human IEC line, Caco-2, was cultured in DMEM (4.5g/L Glc) supplemented with 10% heat-inactivated fetal calf serum, 2 mmol/L glutamine, 100 IU/mL penicillin and 100 µg/mL streptomycin.

Stable Caco-2 cell lines expressing short hairpin RNA (shRNA) sequences targeting ZO-1 or degenerated sequences (control) were established to assess the role of ZO-1. Lentiviral particles (sc-29829-V) were purchased and used according the manufacturer's instructions (Santa Cruz Biotechnology). Stable cell lines were selected in 1 mg/mL puromycin dihydrochloride 2 weeks before use, and maintained under selection during the experimental period. Antibiotic-resistant cell lines were screened by immunoblotting. TEER and permeability were measured as explained for the parental Caco-2 cell line.

Spreading and proliferation assessment

For spreading and proliferation experiments, 60,000 Caco-2 cells were seeded on 12-well Transwell filters (pore size 0.40 µm, Corning, Avon, France). 5-HETE (100 pg/mL) or 15-HETE (100 pg/mL) were added or not the following day for a further 2 days. The IEC size was measured by anti-zonula occludens-1 (ZO-1) immunostaining. After the 2 days of the experiment, IEC Transwell filters were fixed, separated from the Transwell and incubated for 30 min at RT with PBS containing 0.5% Triton X-100 and 10% horse serum (PBS-TX-HS). Filters were then incubated with a mouse monoclonal antibody, anti-ZO-1 (1:500; Invitrogen), diluted in PBS-TX-HS overnight at 4°C. After washing with PBS, filters were incubated with an anti-mouse CY-3 (1:500; Jackson ImmunoResearch) for 45 min at RT. Filters were mounted on slides for fluorescence microscopy analysis. Images were acquired with a digital camera (Olympus DP 50) coupled to a fluorescence microscope (Olympus IX 50). Cell surface area was measured with ImageJ software. An average of 45.3 +/- 7.3 IEC were analyzed for each experimental condition. The proliferation rate was evaluated by counting DAPI nuclear staining.

Measurement of transepithelial electrical resistance (TEER) and permeability

For TEER and permeability experiments, 100,000 Caco-2 cells were seeded on 24-well Transwell filters coated with collagen I. To determine the effect of EGC-conditioned media or 5- or 15-HETE on IEB resistance, the TEER was measured 1 day after treatment with an EVOM epithelial voltohmmeter (World Precision Instruments, Inc, Sarasota, FL). To determine the effect of EGC-conditioned media or 5- or 15-HETE on IEB permeability, 50 µL apical medium were replaced with 50 µL fluorescein-5.6 sulfonic acid (1 mg/mL; Invitrogen). The fluorescence level of basolateral aliquots (150 µL) was measured every 30 min for a period of 180 min using a fluorimeter (Varioskan, Thermo SA, France). Paracellular permeability was determined by the average of the gradient of change in fluorescence intensity over time, using a linear regression fit model measured in the specimens.

Immunocytochemistry and immunohistochemistry

Human and rat EGC seeded in 48-well plates were fixed in PBS/4% paraformaldehyde (PAF) for 15 min. Immunostaining was performed as described in Suppl Mat 3.

Western blotting

After different time periods of 15-HETE stimulation, the Caco-2 filters were washed with ice-cold PBS and placed into ice-cold RIPA buffer containing with protease inhibitor cocktail (Roche diagnostic) and serine-threonine phosphatase inhibitor cocktail (Sigma). Nuclei and unlyzed cells were removed and samples were processed for electrophoresis using the NuPAGE MES SDS buffer kit (Invitrogen) and separated on 4-12% bis-Tris or 3-8% Tris-acetate gels (NuPAGE, Life Technologies). Proteins were transferred to nitrocellulose membranes with the iBlot™ system (Life Technologies). After blocking, blots were incubated overnight at 4°C with primary antibodies diluted in TBS/ 5% nonfat dry milk for mouse anti-ZO-1 (Thermo Scientific, 1:200), mouse anti-ZO-2 (Life Technologies, 1:200), rabbit anti-occludin (Abcam, 1:250), rabbit anti-JAM-A (Bethyl, 1:500), rabbit anti-claudin 1 (Invitrogen, 1:250), mouse anti-claudin 2 (Life Technologies, 1:200),

rabbit anti-phospho-Thr172-AMPK (P-AMPK), rabbit anti-AMPK, rabbit anti-phospho-p44/p42 (P-ERK), rabbit anti-p44/p42, rabbit anti-phosphoY416Src, rabbit anti-Src (Cell Signaling), anti-phosphotyrosine 4G10Platinum, mouse anti- β -actin (Sigma Aldrich, 1:10,000) and mouse anti-beta-GAPDH (1:1000; Santa Cruz). Immunoblots were probed with the appropriate horseradish peroxidase-conjugated secondary antibodies (Life Technologies) and visualized by chemiluminescence (Clarity Western ECL Substrate, Bio-Rad) using a Gel-Doc imager and the Image Lab Software (Bio-Rad). The value of phosphorylated or total protein immunoreactivity was normalized to the unphosphorylated form or GAPDH immunoreactivity, respectively, and expressed as fold increase relative to the average of control values taken as 1.

Real-time quantitative PCR analysis

Human controls or CD EGC were lysed in RA1 buffer (Macherey-Nagel, Düren, Germany) in order to study mRNA expression as described in Suppl Mat 4.

Animal procedure

For *in vivo* assessment of 15-HETE in IEB permeability, 15-HETE (2 mL of 400 ng/mL in PBS) or 15-lipoxygenase inhibitor 1 (2 mL of 4 μ L/mL in PBS; Cayman chemical) were given to male Sprague-Dawley rats (250 g, Janvier) by two intraperitoneal injections of 1 mL (IP) at a 2-h interval. Four hours after the first IP, animals were sacrificed and the entire colon was removed, opened and washed three times in cold Krebs's solution (0.187 g/L $\text{NaH}_2\text{PO}_4 \cdot 2\text{H}_2\text{O}$, 6.84 g/L NaCl, 0.35 g/L KCl, 2.10 g/L NaHCO_3 , 1.98 g/L glucose, 0.368 g/L $\text{CaCl}_2 \cdot 2\text{H}_2\text{O}$, 0.244 g/L $\text{MgCl}_2 \cdot 6\text{H}_2\text{O}$). Four pieces of each colon were mounted in Ussing chambers (0.03 cm^2 exposed surface area) (Physiological instruments, San Diego, CA, USA) as previously described²². Each chamber contained 2 mL Ham's Nutrient Mixture (HAM/F12; Invitrogen, Courtaboeuf, France). The medium was maintained at 37°C under an atmosphere of 95% O_2 and 5% CO_2 . After 30 min of equilibrium, 200 μ L apical medium were replaced with 200 μ L fluorescein-5.6 sulfonic acid (1 mg/mL; Invitrogen). The fluorescence level of basolateral aliquots (150 μ L) was measured every 30 min for a period of 180 min using a fluorimeter (Varioskan, Thermo SA, France). Paracellular permeability was determined by the average of the gradient of change in fluorescence intensity over time, using a linear regression fit model measured in the specimens (GraphPad Software Company, La Jolla, CA, USA). Four rats were included in each group. Two rats of the control group were treated with the 15-HETE excipient, ethanol, whereas two other control rats were treated with the 15-LOX inhibitor excipient, chloroform, at the same dilution as the drugs.

Drugs

5- or 15-HETE were purchased from Cayman Chemicals. U0126 (MEK1/2 inhibitor, 10 μ M; Calbiochem) or AICAR (AMPK activator, 10 μ M; Calbiochem) were added, or not, 30 min prior to the addition of 15-HETE.

Statistical analysis

All graphics were drawn and analyzed with GraphPad Prism Software (GraphPad Software, San Diego, California) using a Kruskal-Wallis nonparametric ANOVA test followed by Dunn's post test. Values of $p \leq 0.05$ were considered statistically significant.

Results

Rat EGC produce 5- and 15-HETE

To uncover molecules potentially implicated in glial-epithelial communication, we characterized the profile of 29 n-6 (eicosanoids)/n-3 (docosanoids) PUFA-derived metabolites in conditioned media of primary cultures of rat EGC (ROG) or rat cell line (JUG). 5- and 15-HETE levels were significantly higher in conditioned media of ROG and JUG compared with defined DMEM culture media (Figure 1). 8-HETE, 18-HEPE, 8isoPGA2, 14-HDoHE, LxA4, PGE2 and TxB2 levels were also significantly higher in ROG-conditioned media, but not in those conditioned with JUG (Figure 1). Among the 29 lipidic mediators analyzed, 5 were undetected, and 15 others did not show any

significant differences compared to defined DMEM culture media (Suppl Mat 1). This analysis showed that rat EGC cell line or primary cultures can produce 5- and 15-HETE.

15-HETE increases IEB spreading and resistance and decreases IEB permeability

In a first set of experiments, we determined if these two mediators could regulate IEB properties by directly treating Caco-2 with 5- or 15-HETE. Compared with untreated cells, 15-HETE significantly increased the TEER (Figure 2A) and decreased the permeability (Figure 2B) of Caco-2 monolayers, whereas 5-HETE had no significant effect. Both mediators increased Caco-2 spreading (Figure 2C) compared with untreated cells. 5- or 15-HETE did not modify Caco-2 cell numbers in these conditions (Figure 2D). These first functional data demonstrate that 5- or 15-HETE could regulate IEB properties, and that 15-HETE had a broader effect than 5-HETE, regulating spreading and also resistance and permeability of an IEC monolayer. We thus focused our study on the effects of 15-HETE.

Human and rat EGC express the 15-lipoxygenase-2

To better understand 15-HETE production by EGC, we used immunostaining to analyze the expression of the two enzymes, 15-lipoxygenase-1 (15-LOX-1) and 15-lipoxygenase-2 (15-LOX-2), responsible for its production in ROG, and also in human EGC and human submucosal plexus. 15-LOX-2 immunoreactivity appeared as a cytoplasmic staining for 100% of ROG (Figure 3A) and human EGC (Figure 3B). 15-LOX-1 immunoreactivity was undetectable. Co-staining of human enteric submucosal plexus with 15-LOX-2 and S100 β glial marker showed that 15-LOX-2 is expressed *in situ* in EGC, and also in neurons (Figure 3C).

Defect of 15-HETE production by CD EGC is responsible for increased IEB permeability

To analyze the importance of glial 15-HETE production and its impact on IEB in a pathological context, we studied EGC from CD patients compared with control patients. 15-Lox-2 mRNA (ALox15B) expression was measured in control and CD EGC and 15-HETE production was measured in control and CD EGC-conditioned media. Whereas ALox15B was expressed at comparable levels in control and CD EGC (Figure 4A), the 15-HETE level was significantly lower in CD compared with control EGC-conditioned media (Figure 4B). To study the functional impact of control and CD EGC on IEB, we replaced Caco-2 basolateral culture media with EGC-conditioned media. Control EGC-conditioned media induced a significant decrease in IEB permeability, but CD EGC-conditioned media had no effect (Figure 4C). 15-HETE supplementation in CD EGC-conditioned media significantly decreased IEB permeability but had no additional effect when added to control EGC-conditioned media (Figure 4C). These data show that the functional defect presented by CD EGC could be fixed by 15-HETE addition.

In vivo inhibition of 15-HETE production induces IEB permeability

To evaluate the range of impact of 15-HETE on IEB permeability *in vivo*, rats were injected i.p. with 15-HETE or 15-LOX inhibitor 1, and the permeability of colon pieces was measured in Ussing chambers. 15-HETE injection had no significant effect, whereas 15-LOX inhibitor 1 injection induced an increase in IEB permeability (Figure 4D). This indicated that 15-HETE production constantly maintains IEB permeability *in vivo*.

15-HETE induces ZO-1 expression in IEC

To further understand the mechanisms of 15-HETE regulation of IEB permeability, we analyzed the expression of tight junction proteins on Caco-2 cells treated with 15-HETE for 5 min, 15 min or 24 h. Expression of the *zonula occludens* 1 (ZO-1) was increased after 15 min and 24 h of 15-HETE treatment, whereas Claudin 1, Claudin 2, occludin, JAM-A and ZO-2 expression were unchanged (Figure 5A and 5B). This indicated that 15-HETE could decrease IEB permeability through a rise in ZO-1 expression.

ZO-1 is necessary to regulate epithelial resistance and permeability in response to 15-HETE

To assess the role of ZO-1 in the effects of 15-HETE, we generated a Caco-2 cell line that downregulates ZO-1 expression. We stably expressed ZO-1 shRNA and isolated a stable cell line on the basis of puromycin resistance. This cell line showed a significant reduction of around 80% of ZO-1 protein levels when compared with control, and no more induction of ZO-1 expression after treatment with 15-HETE (Figure 6A). The 15-HETE-induced increase in TEER and decrease in permeability observed in control Caco-2 were absent in the sh-ZO-1 cell line (Figure 6B and 6C). Compared with control cells, sh-ZO-1 cells presented significantly decreased TEER (Figure 6B) and increased permeability (Figure 6C). These data demonstrate that the regulation of IEB properties by 15-HETE is mediated by ZO-1.

15-HETE inhibits AMPK to increase IEB resistance

To refine the signaling involved in the control of IEB permeability by 15-HETE, we analyzed the transduction pathways that could be activated by 15-HETE in IEC. 15-HETE regulates several cellular functions through tyrosine phosphorylation, Src, ERK or AMPK activation.²³⁻²⁵ Global tyrosine phosphorylation did not vary with the time period of 15-HETE stimulation (Figure 6A and 6B). Quantification of specific major signals of tyrosine phosphorylation at 22, 40 or 110 kDa did not show further variations (quantification not shown). ERK phosphorylation was significantly increased after 15 min and 24 h of 15-HETE treatment, and Src phosphorylation remained stable (Figure 6A and 6B). On the contrary, AMPK phosphorylation was significantly reduced after 15 min of 15-HETE treatment (Figure 6A and 6B). To study the implication of ERK activation or AMPK inhibition on 15-HETE-induced reduction of permeability, we pretreated Caco-2 cells with the ERK pathway inhibitor, U0126, or the AMPK activator, AICAR. U0126 treatment alone decreased IEB permeability, and 15-HETE had no additional effect (Figure 6C). The AICAR compound entirely blocked the 15-HETE-induced decrease in IEB permeability and, despite a trend, had no significant effect alone (Figure 6D). These data demonstrated that ERK activation by 15-HETE was not responsible for the inhibition of IEB permeability by 15-HETE, whereas AMPK inhibition was.

Discussion

Whereas several studies have described phenotypic abnormalities of EGC from CD patients, no functional study is available to define whether these cells present dysfunctions. Our work demonstrates that CD EGC are defective for IEB permeability control, a defect that could be due to their low 15-HETE production. At the same time, we describe how EGC express 15-LOX-2, but not 15-LOX-1, to produce 15-HETE and regulate IEC spreading, IEB resistance and permeability. In addition, 15-HETE controls IEB permeability through AMPK and ZO-1 targeting.

The profile of PUFA derivatives produced by EGC indicates that a few metabolites are present in EGC-conditioned medium, and that LOX metabolites such as 5- and 15-HETE are highly produced, independently of the source of rat EGC, primary cultures or cell lines. Considering the low stability of these compounds, we cannot draw conclusions about the absence of production of the other PUFA by EGC, but we could ensure the production of 5- and 15-HETE. In addition, this study shows for the first time the expression of 15-LOX-2 in human EGC and ganglionated submucosal plexus of the enteric nervous system. Among the 18 LOX sequences published, the 15-LOX-2, originally identified in hair follicles, has been found in skin, prostate, and cornea²⁶, and later in lung, esophageal epithelial cells and ovarian tissue.^{27, 28, 29} The biological functions of 15-LOX-2 in different cell types are diverse. Until now, it has mainly been studied in relation to cancer and atherosclerosis. 15-LOX-2 negatively regulates the proliferation of prostate epithelial cells^{30, 31} and has a tumor suppressing role.^{32, 33} Concerning atherosclerosis, the beneficial role of 15-LOX has for a long while been questioned regarding the anti-inflammatory effect of 15-LOX through lipid mediator production and the proinflammatory and atherogenic effects through oxLDL formation.³⁴ Nevertheless, recent studies have focused on a proatherogenic role of 15-LOX-2³⁵⁻³⁷, in particular by increasing inflammation. In fact, 15-LOX-2 exerts biological activities via the formation of

bioactive lipids, mainly 15-HETE, that could exhibit numerous pro- or anti-inflammatory properties. 15-HETE increases platelet aggregation,³⁸ and induces endothelial cell barrier dysfunction,³⁹ angiogenesis^{24, 40-43} and vascular and pulmonary smooth muscle remodeling.^{23, 25, 44-49} Concerning effects on the epithelium, 15-HETE has been shown to induce cell growth of pre-confluent non-differentiated intestinal epithelial cells.⁵⁰ We did not find an effect of 15-HETE on Caco-2 cell numbers, and could only explain this difference by the confluence and the IEC culture on filters. Only one other study has reported that 15(S)-HETE can increase Caco-2 TEER and decrease permeability⁵¹. We confirmed these results and have additionally shown that 15-HETE induces Caco-2 spreading and controls the permeability *in vivo*. This enlarges the spectrum of the effects of 15-HETE on IEB, and because these are beneficial, we could consider them to reinforce the IEB, especially in a pathological context presenting IEB defects.

Due to their anti- or pro-inflammatory properties, some PUFA have already been measured in the mucosa of inflammatory bowel disease patients.¹⁵⁻¹⁸ More recently, it was shown that levels of PGE₂, PGD₂, TXB₂, 5-HETE, 11-HETE, 12-HETE and 15-HETE were significantly elevated in inflamed mucosa and correlated with the severity of inflammation in UC patients.⁵² 15-HETE production was also induced after ischemia in mouse jejunal tissue.⁵³ Our work provides evidence for a protective role of 15-HETE, prompting a reinforcing of the IEB by diminishing its permeability.

This study additionally shows that, in Caco-2 cells, 15-HETE did not activate Src or induce tyrosine phosphorylation as previously described,^{25, 45} but activated the ERK and inhibited the AMPK pathways. Whereas ERK activation was not responsible for the reduction in permeability observed, the AMPK inhibition was. The energy sensor, AMPK, is generally activated in response to cellular stress, as occurs during inflammation, and to our knowledge few data link 15-LOX activity or 15-HETE production with AMPK. Nevertheless, the nordihydroguaiaretic acid (NDGA) inhibitor of 15-LOX induced phosphorylation and activation of AMPK,⁵⁴ confirming the relation we are describing between 15-HETE and AMPK. In addition, if the expression of AMPK was necessary for an amelioration of the epithelial barrier,^{55, 56} AMPK activation has been linked to intestinal barrier dysfunction.^{57, 58} AMPK activation has also been shown to decrease ZO-1 expression.⁵⁷ Further work is necessary to define if, as described, inhibition of the AMPK alpha2 isoform, but not inhibition of alpha1, can reinforce the epithelial barrier.⁵⁹

Nevertheless, we have shown that the impact of 15-HETE on permeability requires ZO-1 expression, confirming that this tight junction protein is a key mediator of the EGC control of epithelial permeability and resistance^{9, 11, 12, 60}. Taking into account the impact of nutrients and microbiota on the phenotype and function of the enteric nervous system⁶¹, we might wonder whether nutritional status can influence gut wall integrity through the ENS⁶².

Our work defines the novel protective role of 15-HETE on the IEB, and shows that 15-HETE mediates its effect through AMPK inhibition and ZO-1 expression. In addition, this work brings the first evidence of human EGC dysfunction in CD. Overall, our *ex vivo* functional studies indicate that primary cultures of EGC isolated from non-inflamed intestine of CD patients exhibit loss of function as compared with EGC isolated from control patients. These findings suggest that CD EGC have an altered intrinsic functional phenotype. It is thus tempting to speculate that impaired intrinsic functions of EGC from CD patients predispose to and/or directly participate in the disease onset, supporting the idea that CD could be a “gliopathy”.

References

1. Bush TG, Savidge TC, Freeman TC, Cox HJ, Campbell EA, Mucke L, Johnson MH, Sofroniew MV. Fulminant jejuno-ileitis following ablation of enteric glia in adult transgenic mice. *Cell* 1998;93:189-201.
2. **Cornet A, Savidge TC**, Cabarrocas J, Deng WL, Colombel JF, Lassmann H, Desreumaux P, Liblau RS. Enterocolitis induced by autoimmune targeting of enteric glial cells: a possible mechanism in Crohn's disease? *Proc Natl Acad Sci U S A* 2001;98:13306-11.
3. **Aube AC, Cabarrocas J**, Bauer J, Philippe D, Aubert P, Doulay F, Liblau R, Galmiche JP, Neunlist M. Changes in enteric neurone phenotype and intestinal functions in a transgenic mouse model of enteric glia disruption. *Gut* 2006;55:630-7.
4. Arrieta MC, Madsen K, Doyle J, Meddings J. Reducing small intestinal permeability attenuates colitis in the IL10 gene-deficient mouse. *Gut* 2009;58:41-8.
5. Neunlist M, Van Landeghem L, Mahe MM, Derkinderen P, des Varannes SB, Rolli-Derkinderen M. The digestive neuronal-glia-epithelial unit: a new actor in gut health and disease. *Nat Rev Gastroenterol Hepatol* 2013;10:90-100.
6. **Neunlist M, Aubert P**, Bonnaud S, Van Landeghem L, Coron E, Wedel T, Naveilhan P, Ruhl A, Lardeux B, Savidge T, Paris F, Galmiche JP. Enteric glia inhibit intestinal epithelial cell proliferation partly through a TGF-beta1-dependent pathway. *Am J Physiol Gastrointest Liver Physiol* 2007;292:G231-41.
7. **Bach-Ngohou K, Mahe MM**, Aubert P, Abdo H, Boni S, Bourreille A, Denis MG, Lardeux B, Neunlist M, Masson D. Enteric glia modulate epithelial cell proliferation and differentiation through 15-deoxy-12,14-prostaglandin J2. *J Physiol* 2010;588:2533-44.
8. Van Landeghem L, Chevalier J, Mahe MM, Wedel T, Urvil P, Derkinderen P, Savidge T, Neunlist M. Enteric glia promote intestinal mucosal healing via activation of focal adhesion kinase and release of proEGF. *Am J Physiol Gastrointest Liver Physiol* 2011;300:G976-87.
9. Savidge TC, Newman P, Pothoulakis C, Ruhl A, Neunlist M, Bourreille A, Hurst R, Sofroniew MV. Enteric glia regulate intestinal barrier function and inflammation via release of S-nitrosoglutathione. *Gastroenterology* 2007;132:1344-58.
10. Cheadle GA, Costantini TW, Lopez N, Bansal V, Eliceiri BP, Coimbra R. Enteric glia cells attenuate cytomix-induced intestinal epithelial barrier breakdown. *PLoS One* 2013;8:e69042.
11. Costantini TW, Krzyzaniak M, Cheadle GA, Putnam JG, Hageny AM, Lopez N, Eliceiri BP, Bansal V, Coimbra R. Targeting alpha-7 Nicotinic Acetylcholine Receptor in the Enteric Nervous System: A Cholinergic Agonist Prevents Gut Barrier Failure after Severe Burn Injury. *Am J Pathol* 2012;181:478-86.
12. Flamant M, Aubert P, Rolli-Derkinderen M, Bourreille A, Neunlist MR, Mahe MM, Meurette G, Marteyn B, Savidge T, Galmiche JP, Sansonetti PJ, Neunlist M. Enteric glia protect against *Shigella flexneri* invasion in intestinal epithelial cells: a role for S-nitrosoglutathione. *Gut* 2011;60:473-84.
13. von Boyen GB, Schulte N, Pfluger C, Spaniol U, Hartmann C, Steinkamp M. Distribution of enteric glia and GDNF during gut inflammation. *BMC Gastroenterol* 2011;11:3.
14. Jupp J, Hillier K, Elliott DH, Fine DR, Bateman AC, Johnson PA, Cazaly AM, Penrose JF, Sampson AP. Colonic expression of leukotriene-pathway enzymes in inflammatory bowel diseases. *Inflamm Bowel Dis* 2007;13:537-46.
15. Hommes DW, Meenan J, de Haas M, ten Kate FJ, von dem Borne AE, Tytgat GN, van Deventer SJ. Soluble Fc gamma receptor III (CD 16) and eicosanoid concentrations in gut lavage fluid from patients with inflammatory bowel disease: reflection of mucosal inflammation. *Gut* 1996;38:564-7.
16. Sharon P, Stenson WF. Enhanced synthesis of leukotriene B4 by colonic mucosa in inflammatory bowel disease. *Gastroenterology* 1984;86:453-60.
17. Rampton DS, Sladen GE, Youlten LJ. Rectal mucosal prostaglandin E2 release and its relation to disease activity, electrical potential difference, and treatment in ulcerative colitis. *Gut* 1980;21:591-6.
18. Nielsen OH, Ahnfelt-Ronne I, Elmgreen J. Abnormal metabolism of arachidonic acid in chronic inflammatory bowel disease: enhanced release of leukotriene B4 from activated neutrophils. *Gut* 1987;28:181-5.

19. Murakami M, Ohta T, Otsuguro KI, Ito S. Involvement of prostaglandin E(2) derived from enteric glial cells in the action of bradykinin in cultured rat myenteric neurons. *Neuroscience* 2007;145:642-53.
20. Soret R, Coquenlorge S, Cossais F, Meurette G, Rolli-Derkinderen M, Neunlist M. Characterization of human, mouse, and rat cultures of enteric glial cells and their effect on intestinal epithelial cells. *Neurogastroenterol Motil* 2013;25:e755-64.
21. **Le Faouder P, Baillif V**, Spreadbury I, Motta JP, Rousset P, Chene G, Guigne C, Terce F, Vanner S, Vergnolle N, Bertrand-Michel J, Dubourdeau M, Cenac N. LC-MS/MS method for rapid and concomitant quantification of pro-inflammatory and pro-resolving polyunsaturated fatty acid metabolites. *J Chromatogr B Analyt Technol Biomed Life Sci* 2013;932:123-33.
22. De Quelen F, Chevalier J, Rolli-Derkinderen M, Mourot J, Neunlist M, Boudry G. n-3 polyunsaturated fatty acids in the maternal diet modify the postnatal development of nervous regulation of intestinal permeability in piglets. *J Physiol* 2011;589:4341-52.
23. **Jiang J, Wang S**, Wang Z, Ma J, Liu S, Li W, Zhu D. The role of ERK1/2 in 15-HETE-inhibited apoptosis in pulmonary arterial smooth muscle cells. *J Recept Signal Transduct Res* 2011;31:45-52.
24. Kundumani-Sridharan V, Niu J, Wang D, Van Quyen D, Zhang Q, Singh NK, Subramani J, Karri S, Rao GN. 15(S)-hydroxyicosatetraenoic acid-induced angiogenesis requires Src-mediated Egr-1-dependent rapid induction of FGF-2 expression. *Blood* 2010;115:2105-16.
25. Singh NK, Wang D, Kundumani-Sridharan V, Van Quyen D, Niu J, Rao GN. 15-Lipoxygenase-1-enhanced Src-Janus kinase 2-signal transducer and activator of transcription 3 stimulation and monocyte chemoattractant protein-1 expression require redox-sensitive activation of epidermal growth factor receptor in vascular wall remodeling. *J Biol Chem* 2011;286:22478-88.
26. Brash AR, Boeglin WE, Chang MS. Discovery of a second 15S-lipoxygenase in humans. *Proc Natl Acad Sci U S A* 1997;94:6148-52.
27. Chanez P, Bonnans C, Chavis C, Vachier I. 15-lipoxygenase: a Janus enzyme? *Am J Respir Cell Mol Biol* 2002;27:655-8.
28. Xu XC, Shappell SB, Liang Z, Song S, Menter D, Subbarayan V, Iyengar S, Tang DG, Lippman SM. Reduced 15S-lipoxygenase-2 expression in esophageal cancer specimens and cells and upregulation in vitro by the cyclooxygenase-2 inhibitor, NS398. *Neoplasia* 2003;5:121-7.
29. Roffeis J, Hornung D, Kuhn H, Walther M. 15-Lipoxygenase-2 is differentially expressed in normal and neoplastic ovary. *Eur J Cancer Prev* 2007;16:568-75.
30. **Tang DG, Bhatia B**, Tang S, Schneider-Broussard R. 15-lipoxygenase 2 (15-LOX2) is a functional tumor suppressor that regulates human prostate epithelial cell differentiation, senescence, and growth (size). *Prostaglandins Other Lipid Mediat* 2007;82:135-46.
31. Tang S, Bhatia B, Maldonado CJ, Yang P, Newman RA, Liu J, Chandra D, Traag J, Klein RD, Fischer SM, Chopra D, Shen J, Zhau HE, Chung LW, Tang DG. Evidence that arachidonate 15-lipoxygenase 2 is a negative cell cycle regulator in normal prostate epithelial cells. *J Biol Chem* 2002;277:16189-201.
32. Bhatia B, Maldonado CJ, Tang S, Chandra D, Klein RD, Chopra D, Shappell SB, Yang P, Newman RA, Tang DG. Subcellular localization and tumor-suppressive functions of 15-lipoxygenase 2 (15-LOX2) and its splice variants. *J Biol Chem* 2003;278:25091-100.
33. Jiang WG, Watkins G, Douglas-Jones A, Mansel RE. Reduction of isoforms of 15-lipoxygenase (15-LOX)-1 and 15-LOX-2 in human breast cancer. *Prostaglandins Leukot Essent Fatty Acids* 2006;74:235-45.
34. Wittwer J, Hersberger M. The two faces of the 15-lipoxygenase in atherosclerosis. *Prostaglandins Leukot Essent Fatty Acids* 2007;77:67-77.
35. Magnusson LU, Lundqvist A, Karlsson MN, Skalen K, Levin M, Wiklund O, Boren J, Hulthen LM. Arachidonate 15-lipoxygenase type B knockdown leads to reduced lipid accumulation and inflammation in atherosclerosis. *PLoS One* 2012;7:e43142.
36. Wuest SJ, Crucet M, Gemperle C, Loretz C, Hersberger M. Expression and regulation of 12/15-lipoxygenases in human primary macrophages. *Atherosclerosis* 2012;225:121-7.
37. Rydberg EK, Krettek A, Ullstrom C, Ekstrom K, Svensson PA, Carlsson LM, Jonsson-Rylander AC, Hansson GI, McPheat W, Wiklund O, Ohlsson BG, Hulthen LM. Hypoxia increases LDL oxidation and

- expression of 15-lipoxygenase-2 in human macrophages. *Arterioscler Thromb Vasc Biol* 2004;24:2040-5.
38. Vijil C, Hermansson C, Jeppsson A, Bergstrom G, Hulten LM. Arachidonate 15-lipoxygenase enzyme products increase platelet aggregation and thrombin generation. *PLoS One* 2014;9:e88546.
 39. **Othman A, Ahmad S**, Megyerdi S, Mussell R, Choksi K, Maddipati KR, Elmarakby A, Rizk N, Al-Shabrawey M. 12/15-Lipoxygenase-derived lipid metabolites induce retinal endothelial cell barrier dysfunction: contribution of NADPH oxidase. *PLoS One* 2013;8:e57254.
 40. **Ma C, Li Y, Ma J**, Liu Y, Li Q, Niu S, Shen Z, Zhang L, Pan Z, Zhu D. Key role of 15-lipoxygenase/15-hydroxyeicosatetraenoic acid in pulmonary vascular remodeling and vascular angiogenesis associated with hypoxic pulmonary hypertension. *Hypertension* 2011;58:679-88.
 41. Soumya SJ, Binu S, Helen A, Anil Kumar K, Reddanna P, Sudhakaran PR. Effect of 15-lipoxygenase metabolites on angiogenesis: 15(S)-HPETE is angiostatic and 15(S)-HETE is angiogenic. *Inflamm Res* 2012;61:707-18.
 42. Soumya SJ, Binu S, Helen A, Reddanna P, Sudhakaran PR. 15(S)-HETE-induced angiogenesis in adipose tissue is mediated through activation of PI3K/Akt/mTOR signaling pathway. *Biochem Cell Biol* 2014;91:498-505.
 43. **Yuan D, Ran Y**, Liu Q, Zhang Y, Li H, Li P, Zhu D. Enhancement of the HIF-1 α /15-LO/15-HETE axis promotes hypoxia-induced endothelial proliferation in preeclamptic pregnancy. *PLoS One* 2014;9:e96510.
 44. **Li X, Ma C**, Zhu D, Meng L, Guo L, Wang Y, Zhang L, Li Z, Li E. Increased expression and altered subcellular distribution of PKC- δ and PKC- ϵ in pulmonary arteries exposed to hypoxia and 15-HETE. *Prostaglandins Other Lipid Mediat* 2010;93:84-92.
 45. **Potula HS, Wang D**, Quyen DV, Singh NK, Kundumani-Sridharan V, Karpurapu M, Park EA, Glasgow WC, Rao GN. Src-dependent STAT-3-mediated expression of monocyte chemoattractant protein-1 is required for 15(S)-hydroxyeicosatetraenoic acid-induced vascular smooth muscle cell migration. *J Biol Chem* 2009;284:31142-55.
 46. Wang S, Wang Y, Jiang J, Wang R, Li L, Qiu Z, Wu H, Zhu D. 15-HETE protects rat pulmonary arterial smooth muscle cells from apoptosis via the PI3K/Akt pathway. *Prostaglandins Other Lipid Mediat* 2010;91:51-60.
 47. Wang Y, Liang D, Wang S, Qiu Z, Chu X, Chen S, Li L, Nie X, Zhang R, Wang Z, Zhu D. Role of the G-protein and tyrosine kinase--Rho/ROK pathways in 15-hydroxyeicosatetraenoic acid induced pulmonary vasoconstriction in hypoxic rats. *J Biochem* 2010;147:751-64.
 48. **Zhang L, Ma J**, Li Y, Guo L, Ran Y, Liu S, Jiang C, Zhu D. 15-Hydroxyeicosatetraenoic acid (15-HETE) protects pulmonary artery smooth muscle cells against apoptosis via HSP90. *Life Sci* 2010;87:223-31.
 49. **Zhang L, Ma J**, Shen T, Wang S, Ma C, Liu Y, Ran Y, Wang L, Liu L, Zhu D. Platelet-derived growth factor (PDGF) induces pulmonary vascular remodeling through 15-LO/15-HETE pathway under hypoxic condition. *Cell Signal* 2012;24:1931-9.
 50. Cabral M, Martin-Venegas R, Moreno JJ. Role of arachidonic acid metabolites on the control of non-differentiated intestinal epithelial cell growth. *Int J Biochem Cell Biol* 2013;45:1620-8.
 51. Ohata A, Usami M, Miyoshi M. Short-chain fatty acids alter tight junction permeability in intestinal monolayer cells via lipoxygenase activation. *Nutrition* 2005;21:838-47.
 52. **Masoodi M, Pearl DS**, Eiden M, Shute JK, Brown JF, Calder PC, Trebble TM. Altered colonic mucosal Polyunsaturated Fatty Acid (PUFA) derived lipid mediators in ulcerative colitis: new insight into relationship with disease activity and pathophysiology. *PLoS One* 2013;8:e76532.
 53. Gobbetti T, Le Faouder P, Bertrand J, Dubourdeau M, Barocelli E, Cenac N, Vergnolle N. Polyunsaturated fatty acid metabolism signature in ischemia differs from reperfusion in mouse intestine. *PLoS One* 2013;8:e75581.
 54. Lee MS, Kim D, Jo K, Hwang JK. Nordihydroguaiaretic acid protects against high-fat diet-induced fatty liver by activating AMP-activated protein kinase in obese mice. *Biochem Biophys Res Commun* 2010;401:92-7.

55. Elamin EE, Masclee AA, Dekker J, Pieters HJ, Jonkers DM. Short-chain fatty acids activate AMP-activated protein kinase and ameliorate ethanol-induced intestinal barrier dysfunction in Caco-2 cell monolayers. *J Nutr* 2013;143:1872-81.
56. Jing H, Yao J, Liu X, Fan H, Zhang F, Li Z, Tian X, Zhou Y. Fish-oil emulsion (omega-3 polyunsaturated fatty acids) attenuates acute lung injury induced by intestinal ischemia-reperfusion through Adenosine 5'-monophosphate-activated protein kinase-sirtuin1 pathway. *J Surg Res* 2014;187:252-61.
57. Scharl M, Paul G, Barrett KE, McCole DF. AMP-activated protein kinase mediates the interferon-gamma-induced decrease in intestinal epithelial barrier function. *J Biol Chem* 2009;284:27952-63.
58. Scharl M, Paul G, Weber A, Jung BC, Docherty MJ, Hausmann M, Rogler G, Barrett KE, McCole DF. Protection of epithelial barrier function by the Crohn's disease associated gene protein tyrosine phosphatase n2. *Gastroenterology* 2009;137:2030-2040 e5.
59. Qin S, Rodrigues GA. Differential roles of AMPKalpha1 and AMPKalpha2 in regulating 4-HNE-induced RPE cell death and permeability. *Exp Eye Res* 2010;91:818-24.
60. **Neunlist M, Toumi F**, Oreschkova T, Denis M, Leborgne J, Laboisie CL, Galmiche JP, Jarry A. Human ENS regulates the intestinal epithelial barrier permeability and a tight junction-associated protein ZO-1 via VIPergic pathways. *Am J Physiol Gastrointest Liver Physiol* 2003;285:G1028-36.
61. Neunlist M, Schemann M. Nutrient-induced changes in the phenotype and function of the enteric nervous system. *J Physiol* 2014;592:2959-65.
62. Cani PD, Possemiers S, Van de Wiele T, Guiot Y, Everard A, Rottier O, Geurts L, Naslain D, Neyrinck A, Lambert DM, Muccioli GG, Delzenne NM. Changes in gut microbiota control inflammation in obese mice through a mechanism involving GLP-2-driven improvement of gut permeability. *Gut* 2009;58:1091-103.

Author names in bold designate shared co-first authorship

Figures and Figure legends

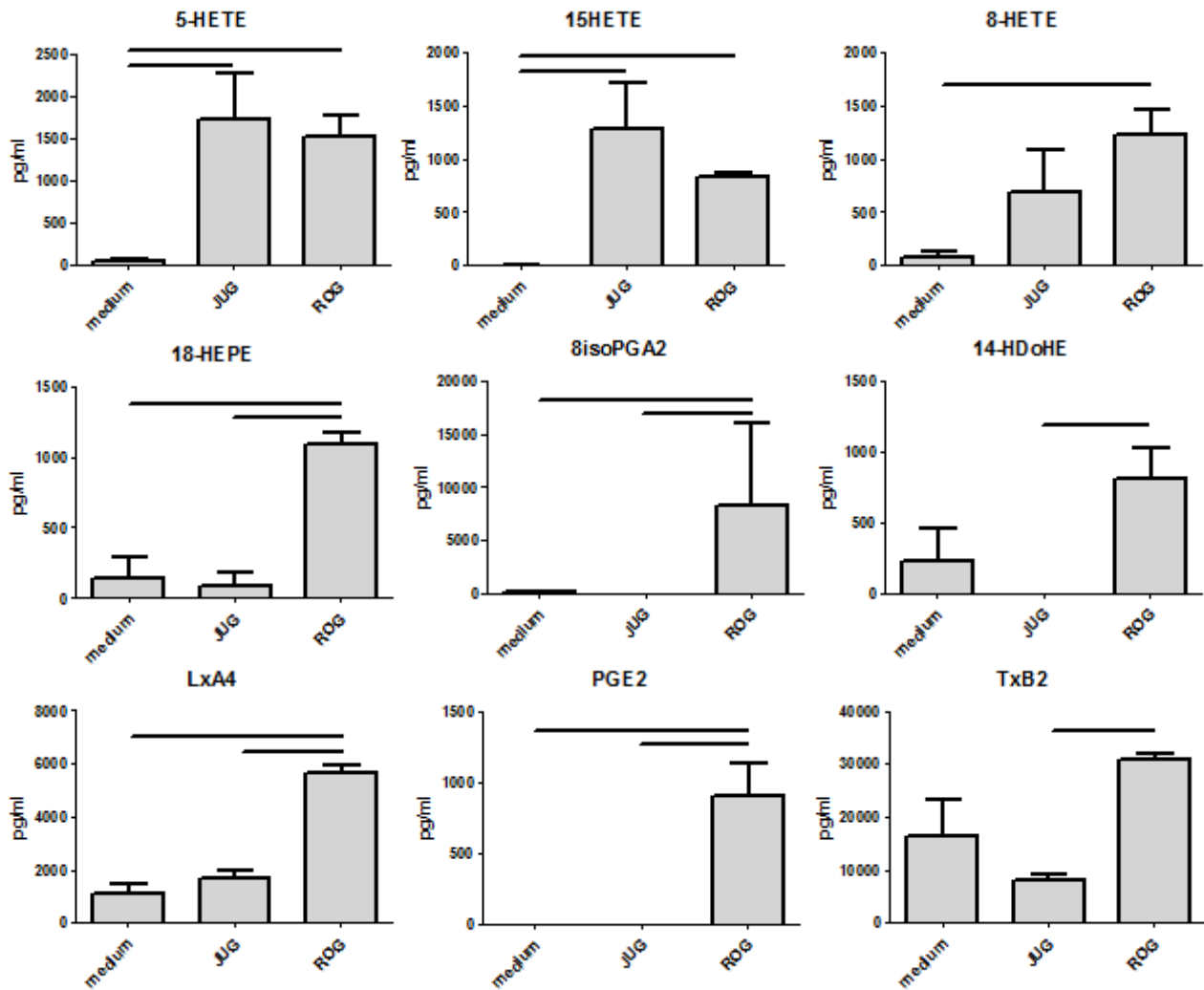


Figure 1

Figure 1. Rat EGC mostly produce 5- and 15-HETE.

Production of eicosanoids by EGC was measured using high sensitivity liquid chromatography tandem mass spectrometry in the culture medium of a rat EGC cell line (JUG) or primary cultures of rat EGC (ROG). Nine compounds were differentially present in culture medium alone (medium) or after 3 days of JUG or ROG culture. Fifteen compounds were present at the same level in these three media, and five compounds were undetected (Suppl Mat 1). Data represent means \pm SEM of 4 independent cultures, $p < 0.05$.

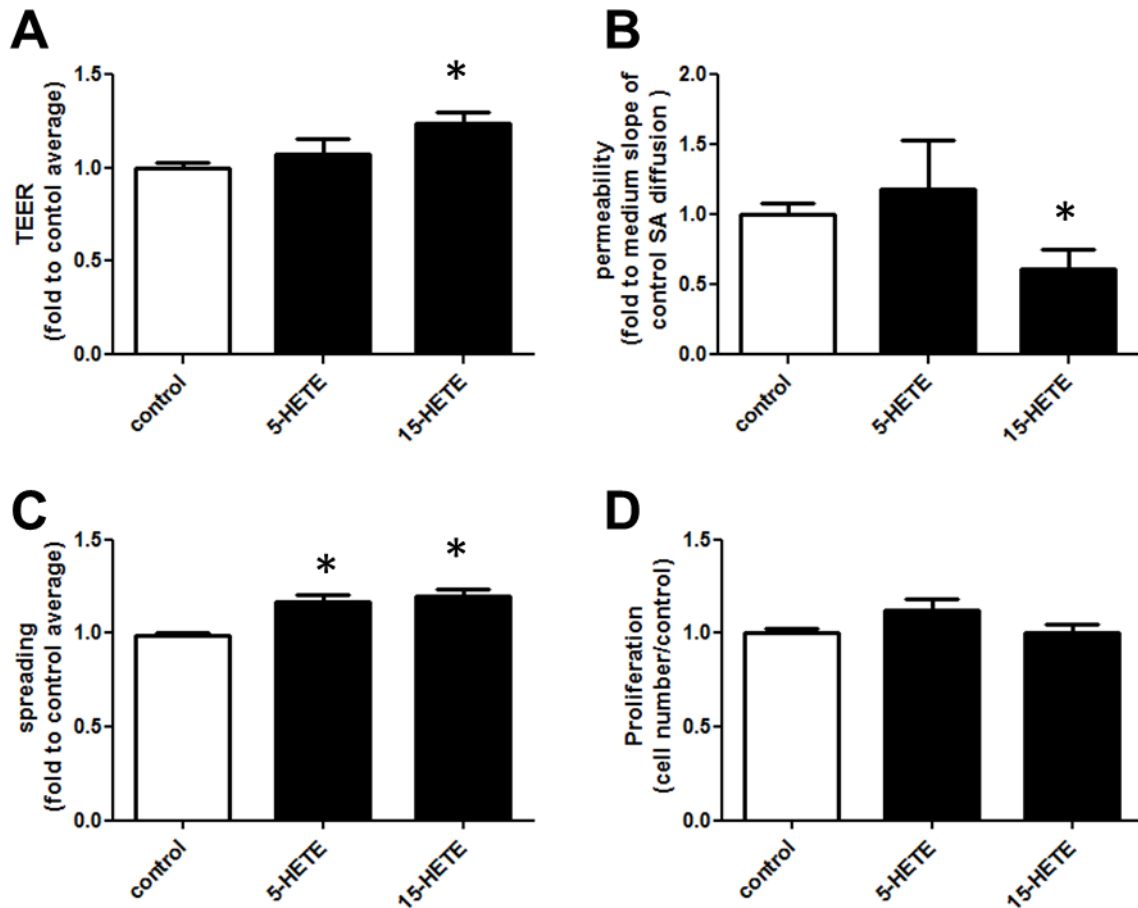


Figure 2

Figure 2. 15-HETE increases IEB spreading and resistance and decreases IEB permeability. 5- or 15-HETE functional impact on IEB was assessed by TEER, permeability, spreading and proliferation measurements. (A) TEER was measured on a Caco-2 monolayer after 1 day of 5- or 15-HETE (100 pg/mL) in the basolateral chamber. (B) Permeability was measured by sulfonic acid flux through the same Caco-2 monolayer. (C) Spreading was measured using ZO-1 staining on Caco-2 after 2 days of treatments. (D) Cell proliferation was estimated by direct counting of DAPI staining. These four parameters are represented as fold to the control average. Data represent means \pm SEM of 4 to 6 independent experiments.* $p < 0.05$.

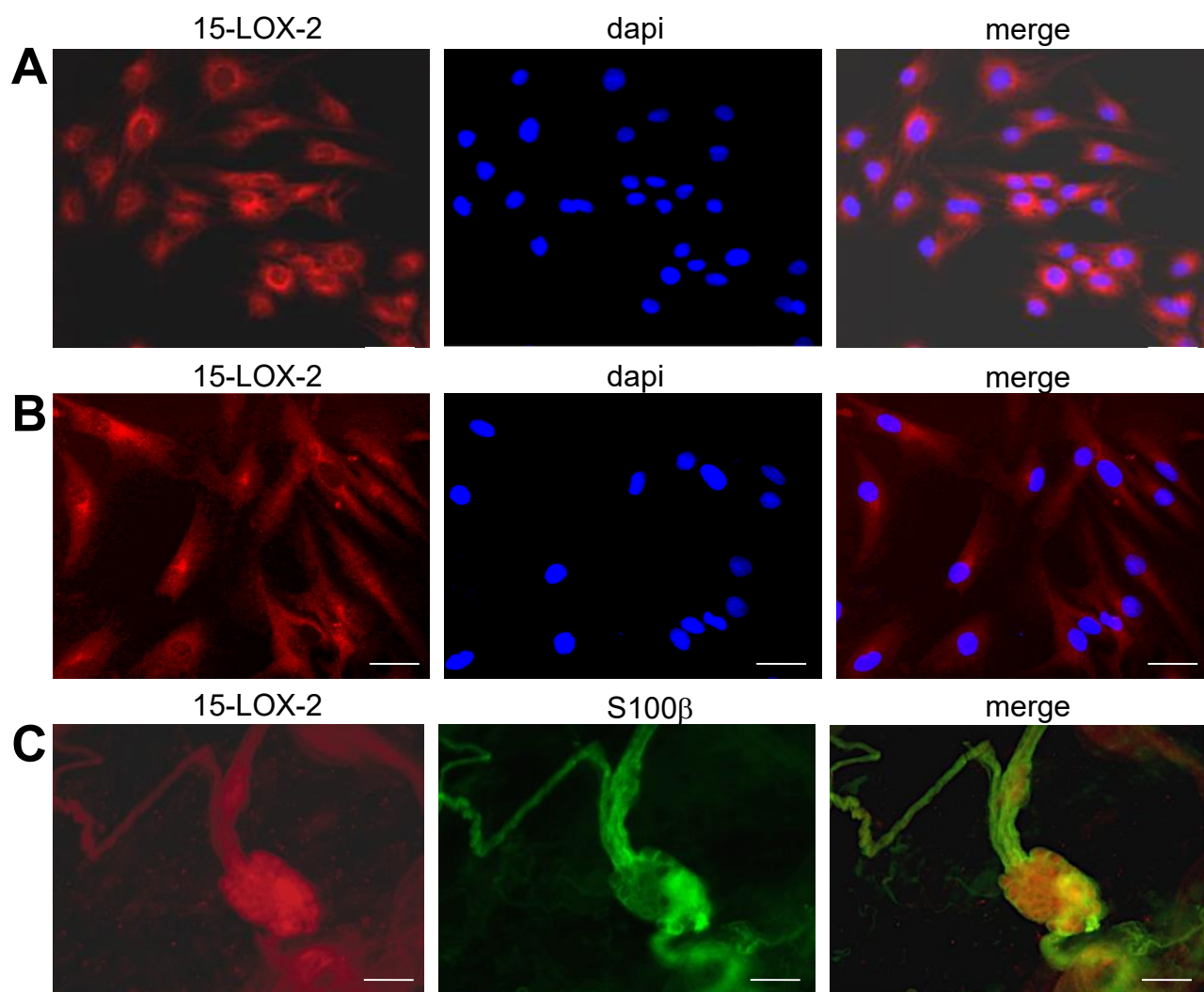


Figure 3

Figure 3. Human and rat EGC express the 15-lipoxygenase-2.

(A) ROG and (B) human EGC immunostaining for 15-lipoxygenase-2 (15-LOX-2). Scale bar, 50 μ m. (C) Submucosal immunohistochemistry was performed using anti-15LOX-2 and -S100 β (glial marker) antibodies. Representative pictures. Scale bar, 100 μ m.

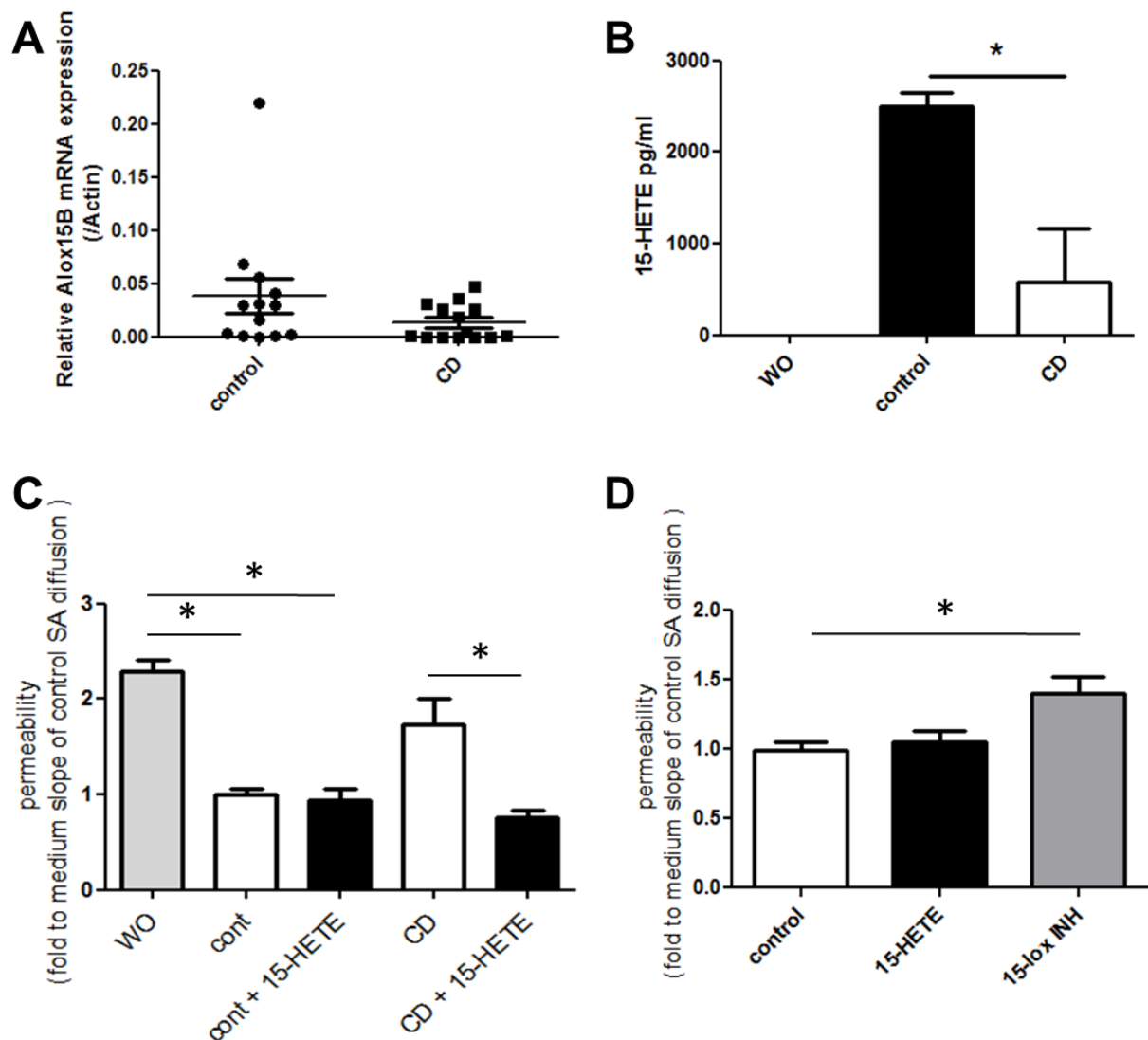


Figure 4

Figure 4. EGC from CD patients are functionally abnormal: they misproduce 15-HETE and fail to reduce IEB permeability.

(A) ALox15B mRNA (coding for 15-LOX-2) expression was measured in human EGC from control (control) or CD (CD) patients. (B) 15-HETE production was measured by liquid chromatography-tandem mass spectrometry in the culture medium of human EGC from control or CD patients, or in the culture medium alone (WO). Data represent means \pm SEM of 6 independent control and 5 CD EGC cultures. * $p < 0.05$. (C) Permeability was measured by sulfonic acid flux through the Caco-2 monolayer incubated without (WO) or with control (cont) or CD (CD) EGC-conditioned media, with supplementation of 15-HETE (+15-HETE) or not. Data represent means \pm SEM of fold to the control average of 3 to 6 independent experiments. * $p < 0.05$. (D) 15-HETE functional impact *in vivo* was evaluated by the measurement of colon permeability of rats 4 h after IP injections with 15-HETE (15-HETE) or 15-lipoxygenase inhibitor 1 (15-lox INH). Data represent means \pm SEM of 2 independent experiments, 4 animals per group for each experiment; * $p < 0.05$.

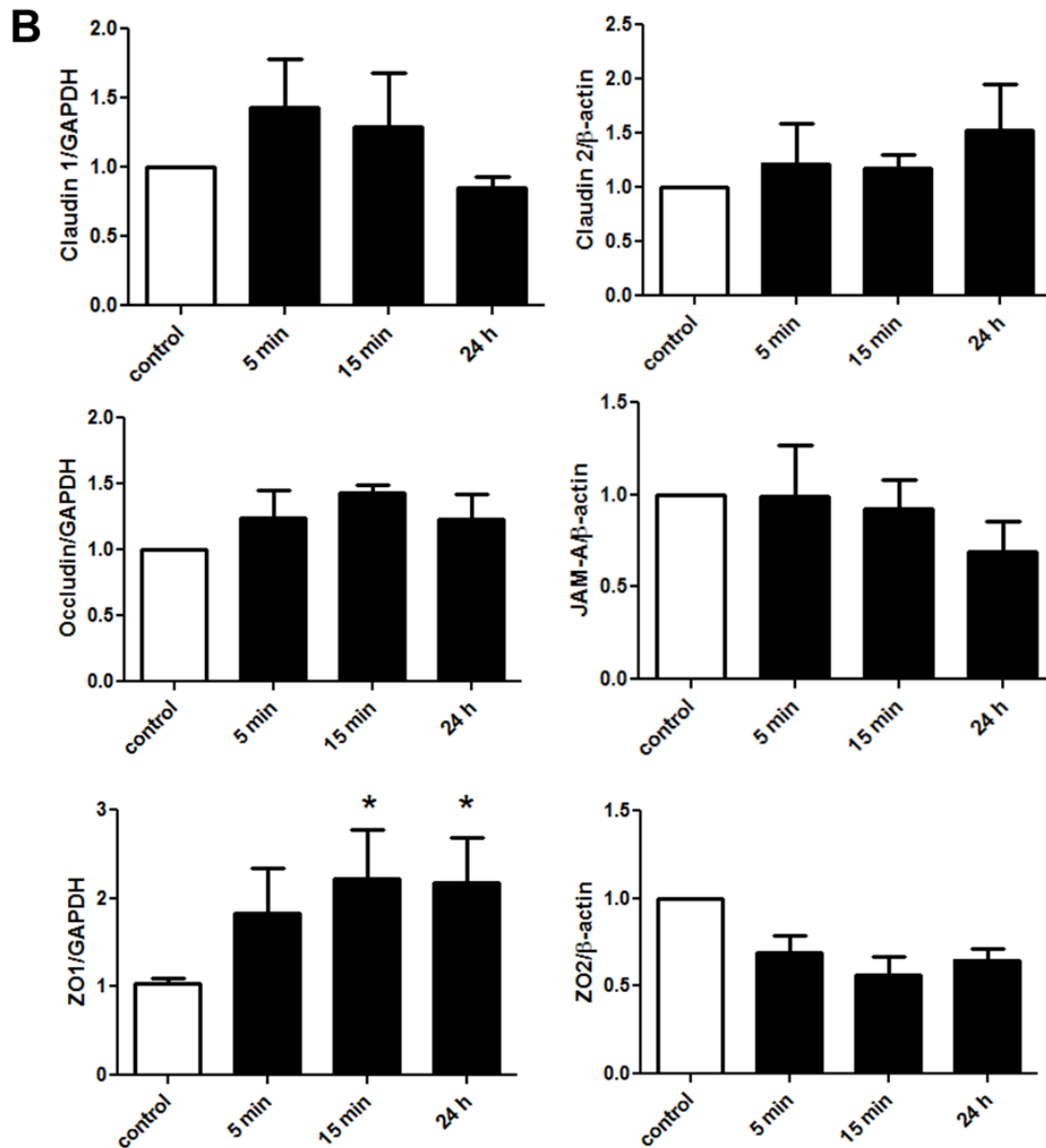
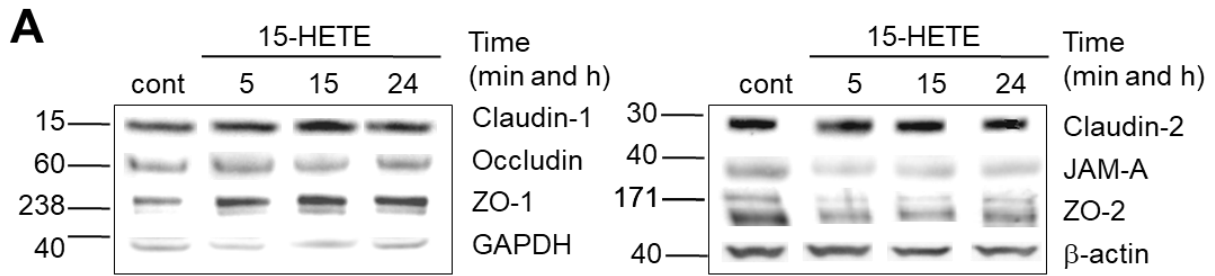


Figure 5

Figure 5. 15-HETE induces ZO-1 expression in IEC.

(A) Claudin-1, Claudin-2, occluding, JAM-A, ZO-1 and ZO-2 expression were measured by western blotting from Caco-2 monolayers stimulated for 5 min, 15 min or 24 h with 15-HETE (100 pg/mL) at the basolateral side. (B) Quantification of western blot analysis. Data represent means of fold to control average \pm SEM of 3 to 4 independent experiments. * $p < 0.05$.

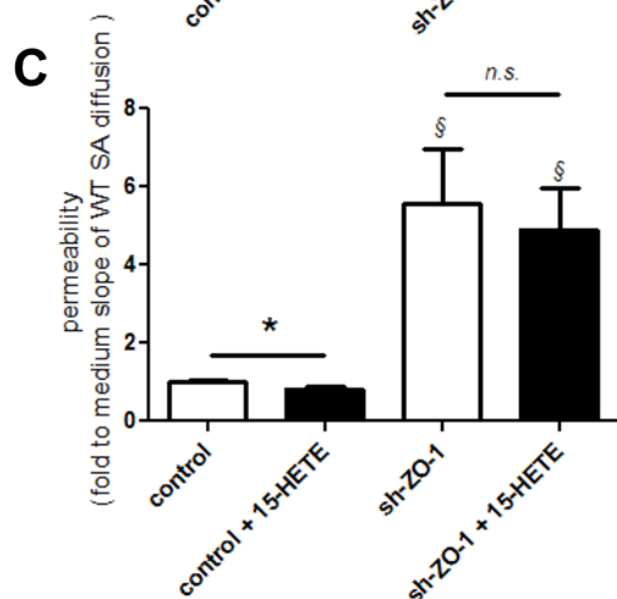
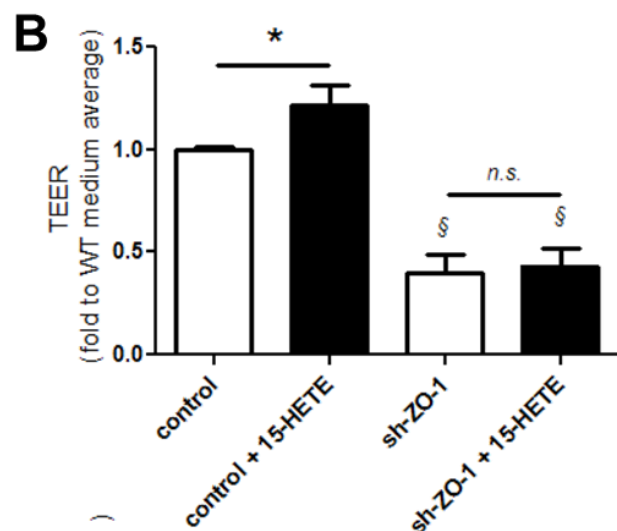
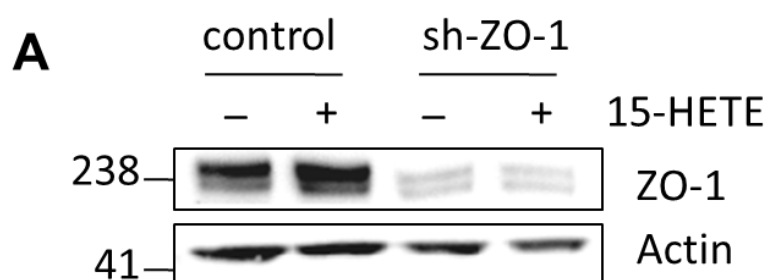


Figure 6

Figure 6. ZO-1 is necessary to regulate epithelial resistance and permeability in response to 15-HETE.

Stable Caco-2 cell lines expressing short hairpin RNA (shRNA) sequences targeting ZO-1 (sh-ZO-1) or degenerated sequences (control) were established to assess the role of ZO-1 in 15-HETE effects. (A) Representative western blot analysis shows that sh-ZO-1 effectively knocks-down ZO-1 expression. (B) TEER was measured on control or sh-ZO-1 Caco-2 monolayers with or without 1 day of 15-HETE (100 pg/mL) in the basolateral chamber. (C) Permeability was measured by sulfonic acid flux through the same Caco-2 monolayers. These two parameters are represented as fold to the medium control average. Data represent means \pm SEM of 6 independent experiments. * $p < 0.05$ compared to without 15-HETE; § $p < 0.05$ compared to control.

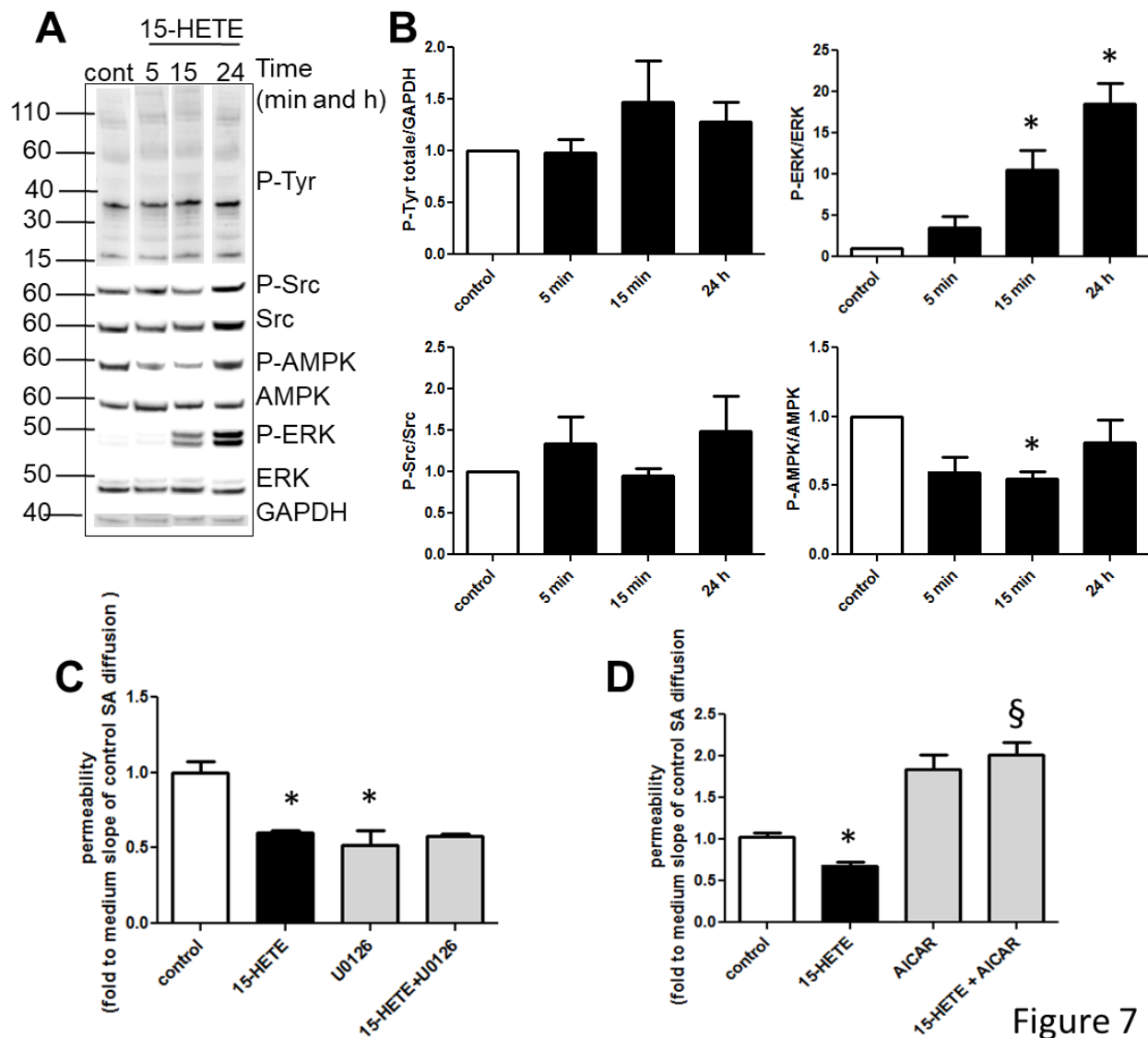


Figure 7

Figure 7. 15-HETE inhibits AMPK to decrease IEB permeability.

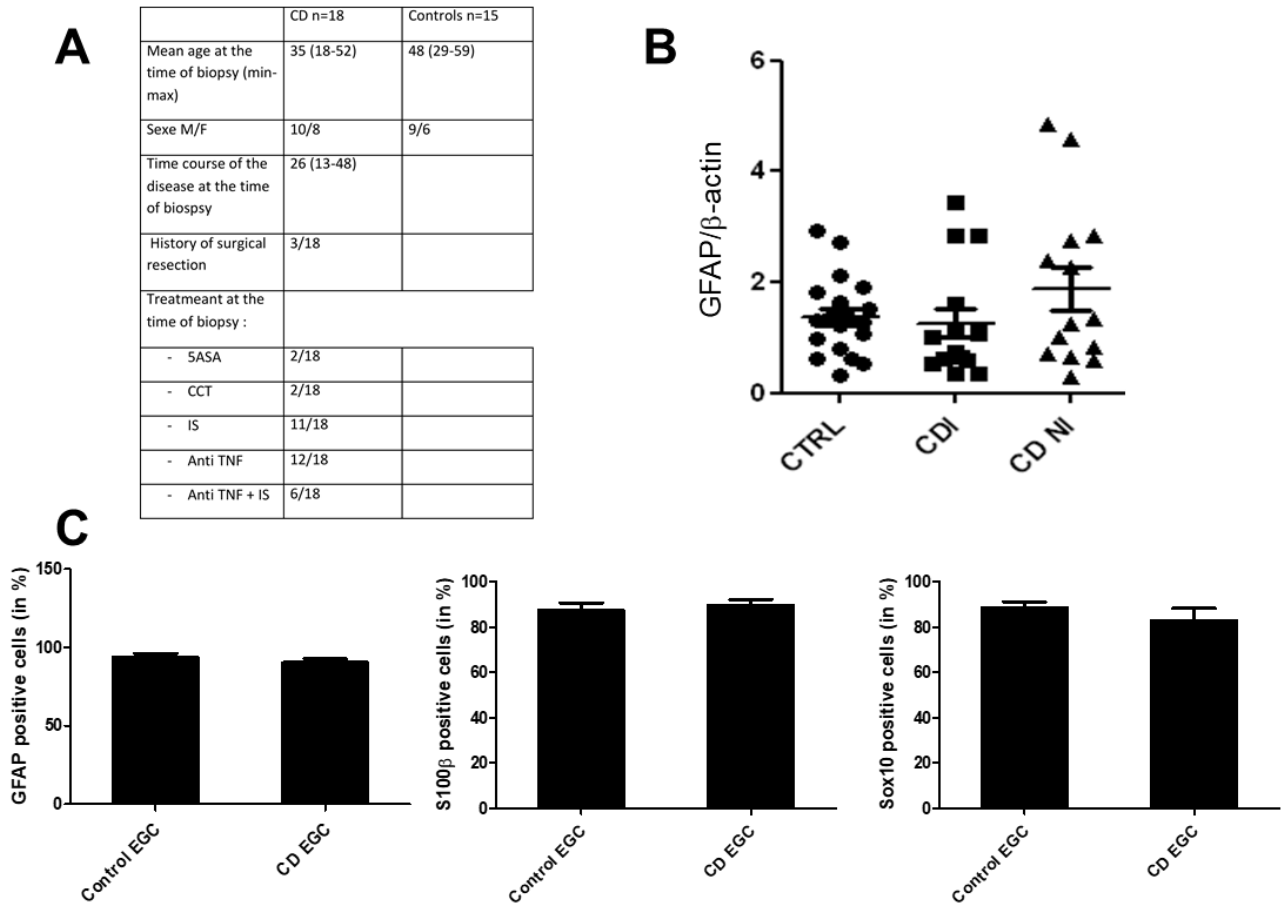
(A) Total phospho-Tyrosine (P-Tyr), ERK phosphorylation (P-ERK), Src phosphorylation (P-Src) and AMPK phosphorylation (P-AMPK) levels were measured by western blotting from Caco-2 monolayers stimulated for 5 min, 15 min or 24 h with 15-HETE (100 pg/mL) at the basolateral side. (B) Quantification of western blot analysis. Data represent means of fold to control average \pm SEM of 4 independent experiments. * $p < 0.05$. (C) Impact of ERK inhibition on IEB permeability was assessed by pretreatment of Caco-2 monolayer with the MEK inhibitor (U0126, 10 μ M) 30 min prior to 15-HETE stimulation. Data represent means of fold to control average \pm SEM of 3 independent experiments. * $p < 0.05$. (D) Impact of AMPK activation on IEB permeability was assessed by treatment of Caco-2 monolayer with the AMPK activator (AICAR, 10 μ M). Data represent means of fold to control average \pm SEM of 3 independent experiments. * $p < 0.05$ vs control; § $p < 0.05$ vs 15-HETE.

		6kPGF1a	PGE3	LxB4	RvDx	LtB5	PGA1	LtB4	15dPGJ2
medium	(pg/ml)	115.82	1250.16	2092.93	1521.20	0.00	0.00	410.42	433.65
	SD	200.60	578.57	1246.22	566.70	0.00	0.00	246.50	195.76
JUG	(pg/ml)	0.00	592.59	1141.71	2099.77	0.00	0.00	389.04	457.11
	SD	0.00	105.39	1141.92	848.34	0.00	0.00	252.29	112.16
ROG	(pg/ml)	1569.05	561.04	356.51	1094.27	138.80	463.47	351.75	395.27
	SD	2813.47	727.60	797.18	265.23	310.38	1036.34	110.24	49.16
		17-HDoHE	12-HETE	14,15-EET	5-oxoETE	11,12-EET	8,9-EET	5,6-EET	ND
medium	(pg/ml)	0.00	292.21	244.21	38584.08	1058.09	0.00	82.54	PGF2a
	SD	0.00	506.13	422.98	24982.21	1832.66	0.00	142.96	RvD1
JUG	(pg/ml)	0.00	1106.24	0.00	32835.13	1503.71	0.00	877.12	7MaR1
	SD	0.00	1424.77	0.00	34447.21	1507.94	0.00	1519.21	PD1
ROG	(pg/ml)	460.90	2434.02	873.64	38223.42	399.85	136.07	381.46	5,6-DIHETE
	SD	654.16	1368.65	906.52	30814.11	894.08	304.26	364.22	

SUPPL MAT 1. Rat EGC mostly produce 5- and 15-HETE.

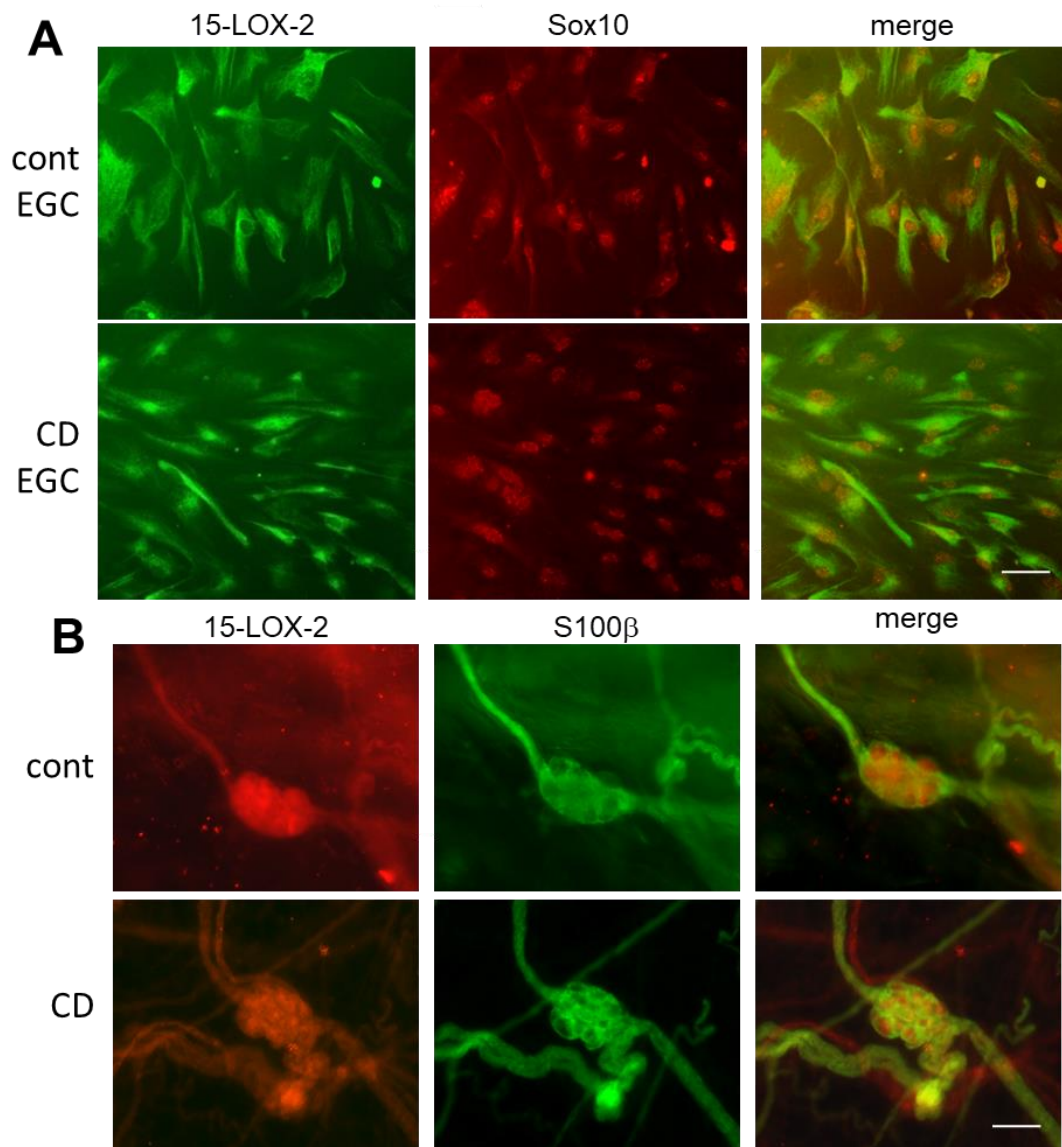
The PUFA dosage was performed as described by Le Faouder et al.²¹ This innovative method allows the simultaneous measurement of 29 lipids: 6-keto-prostaglandin F1 α (6kPGF $_{1\alpha}$); thromboxan B2 (TXB $_2$); prostaglandin E2 (PGE $_2$); prostaglandin E3 (PGE $_3$); prostaglandin A1 (PGA $_1$); 8-iso prostaglandin A2 (8-isoPGA $_2$); 15-Deoxy-Delta12,14-Prostaglandin J2 (15d-PGJ $_2$); lipoxin A4 (LxA $_4$); resolvin D1 (RvD $_1$); leukotrien B4 (LTB $_4$); leukotrien B5 (LTB $_5$); 10(S); 17(S)-protectin (PDx); 18-hydroxyeicosapentaenoic acid (18-HEPE); 15-hydroxyeicosatetraenoic acid (15-HETE), and 12-HETE, 8-HETE, 5-HETE; 17-hydroxy-docosahexaenoic acid (17-HDoHE), and 14-HDoHE; 14,15-epoxyeicosatrienoic acid (14,15-EET), and 11,12-EET, 8,9-EET, 5,6-EET; 5-oxoeicosatetraenoic acid (5-oxo-ETE). Briefly, the 29 lipids of interest and 3 deuterated internal standards (LxA $_4$ -d5, LTB $_4$ -d4, 5-HETE-d8) were separated by LC-MS/MS analysis on an HPLC system (Agilent LC1290 Infinity) coupled to Agilent 6460 triple quadrupole MS (Agilent Technologies) equipped with electrospray ionization operating in negative mode. Reverse-phase HPLC was performed using a ZorBAX SB-C18 column (2.1 mm;50 mm;1.8 μ m) (Agilent Technologies) with a gradient elution. Mobile phase A consisted of water, ACN and FA (75/25/0.1); Solvent B: ACN, FA (100/0.1). Compounds were separated with a linear gradient to 85% B from 0 to 8.5 min and 100% B to 9 min. Isocratic elution continued for 1 min at 100% B then 100% A was reached at 11 min and maintained to 12 min. The flow rate was 0.35 mL/min. The autosampler was set at 5°C and the injection volume was 5 μ L. Data were acquired in MRM mode with optimized conditions (fragmentors and collision energy). Peak detection, integration and quantitative analyses were performed using MassHunter Quantitative Analysis software (Agilent Technologies).

Production of eicosanoids by EGC was measured using high sensitivity liquid chromatography tandem mass spectrometry in the culture medium of a rat EGC cell line (JUG) or primary cultures of rat EGC (ROG). Nine compounds were differentially present in culture medium alone (medium) or after 3 days of JUG or ROG culture (Figure 1). Fifteen compounds were present at the same level in these three media, and five compounds were undetected (ND) (Suppl Mat 1). Data represent means \pm SEM of 4 independent cultures, p<0.05.



SUPPLMAT 2. EGC from CD patients are comparable to EGC from control patients.

(A) Main clinical features of patients with Crohn's disease (CD) and control. 5-aminosalicylic acid (5-ASA); corticoids (CCT); immunosuppressive treatment (IS); anti-Tumor Necrosis Factor alpha antibodies (anti-TNF). (B) GFAP mRNA was quantified in biopsies from control (CTRL) or CD patients in inflamed (CDI) or non inflamed (CD NI) area. (C) Cells expressing the glial markers GFAP, S100 β or Sox10 are expressed as percentage of the total cells in each culture used.

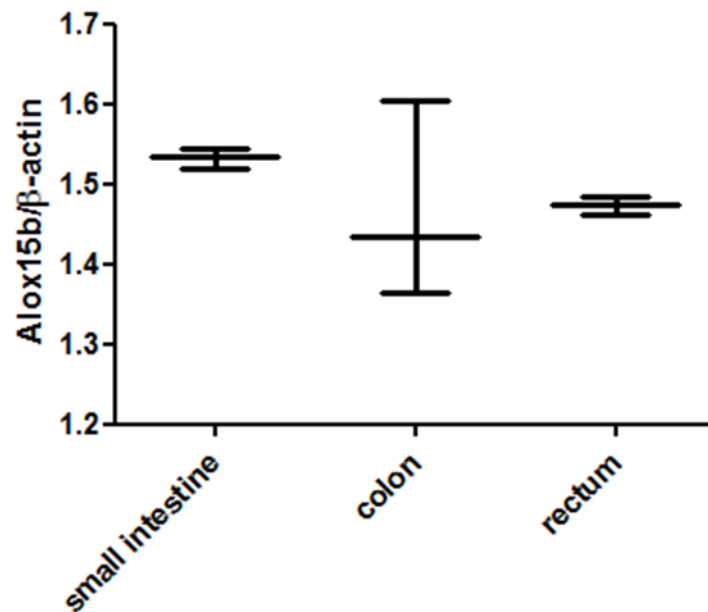


SUPPL MAT 3. Human EGC from control patients (cont EGC) or Crohn's disease patients (CD EGC) express the 15-lipoxygenase-2.

To compare 15-lipoxygenase-2 (15-LOX-2) expression in control (cont EGC) versus CD EGC, we have observed 15-lox2- immunostaining in culture or *in situ*.

Immunostaining was performed using the 15-Lipoxygenase-2 Polyclonal Antibody (1:500; Cayman) or the 15-Lipoxygenase-1 Polyclonal Antibody (1:500; Cayman) and a secondary anti-sheep or anti-rabbit 488 (713-095-147; 1:1000; Jackson ImmunoResearch or FluoProbes®488; 1:1000; Interchim). Submucosal plexuses of control patients were also analyzed for lipoxygenase immunoreactivity with slight modification of time and buffer composition from the protocol described above. Tissues were fixed for 4 h in PAF and incubated in NH₄Cl (100 mM) for 15 min before incubation in PBS-0.5% Triton X-100-1% saponine for 1 h and a blocking procedure for 2 h in PBS-0.5% triton X-100-1% saponin and 10% horse serum. Primary antibodies were incubated for 2 days, and secondary antibodies overnight. S100b (mouse monoclonal antibody, Abcam) immunoreactivity allows the identification of EGC. Images were acquired with an Olympus IX 50 fluorescence microscope coupled to a digital camera (model DP71, Olympus) and analyzed with Cell B software (Soft Imaging System, Olympus).

(A) human EGC immunostaining for 15-LOX-2 or Sox-10 glial marker. Scale bare 50μm. (B) Immunohistochemistry of submucosal plexus from control (cont) or CD patients (CD) was performed using anti-15LOX-2 and -S100β (glial marker) antibodies. Representative pictures. Scale bare 100μm

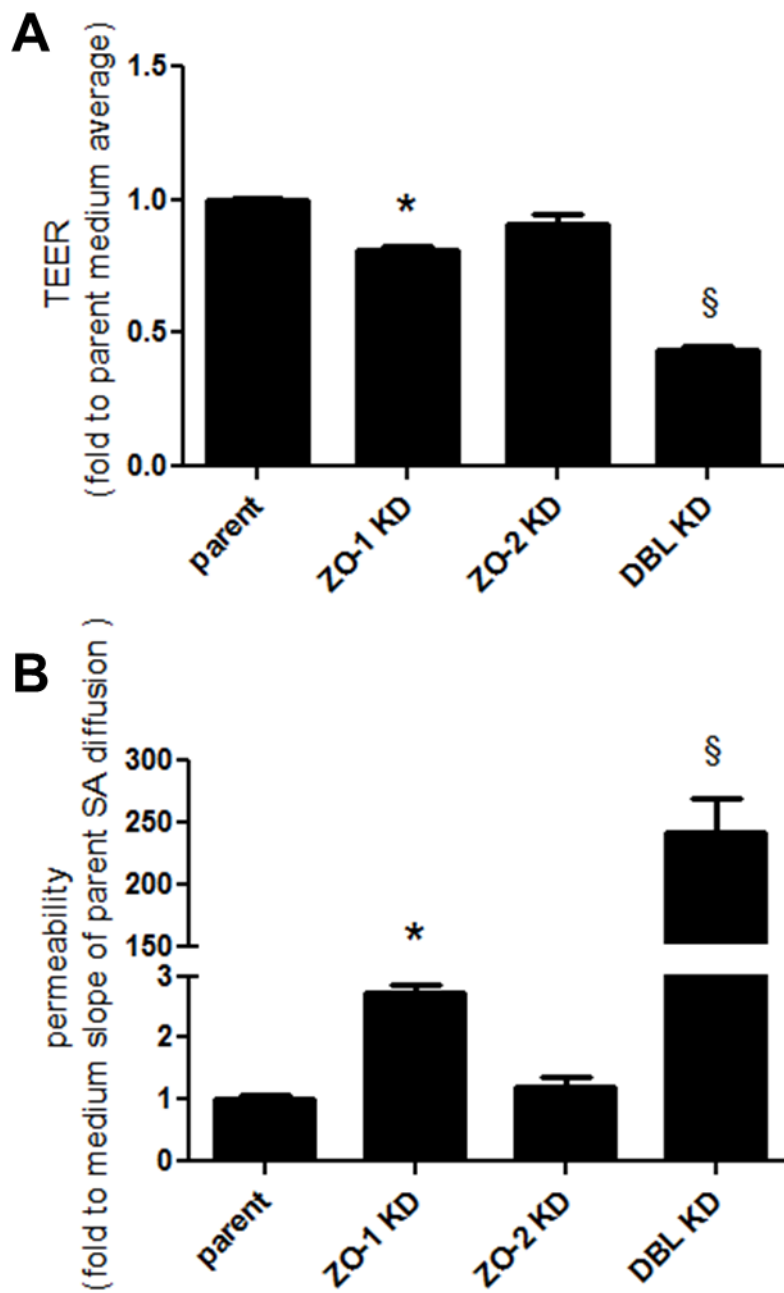


SUPPL MAT 4. ALox15B is expressed all along the gut.

ALox15B mRNA (coding for 15-LOX-2) expression was measured in human small intestine (n=4), colon (n=4) or rectum (n=3).

Following the manufacturer's recommendations, total RNA extraction from cells or tissues was performed with the Nucleospin RNAII kit (Macherey-Nagel) and 1 µg purified RNA was denatured and processed for reverse transcription using Superscript III reverse transcriptase (Invitrogen). PCR amplifications were performed using the Taqman Gene Expression Assay (Life Technologies) and run on a StepOnePlus system (Life Technologies). The following primers were used: b-actin Control kit Yakima (Eurogentec) and Alox15B (Hs00153988_m1, Life Technologies). Relative quantification of gene expression was determined using the standard curve method and endogenous control b-actin mRNA.

SUPPL MAT 4



SUPPLMAT 5. ZO-1 is necessary to regulate epithelial resistance and permeability in MDCK

As opposed to ZO-2, ZO-1 regulates TEER and limits solute permeability. To assess the role of ZO-1 and ZO-2 on TEER and permeability to sulfonic acid, we studied stable Madin-Darby canine kidney (MDCK) II cell lines expressing short hairpin RNA (shRNA) sequences targeting both ZO-1 (ZO-1 KD), ZO-2 (ZO-2 KD) or both ZO-1 and ZO-2 (DBL KD. (A) TEER was measured on parent or KD MDCK monolayer (B) Permeability was measured by sulfonic acid flux through the same MDCK monolayer. These two parameters are represented as fold to the medium parent average. Data represent means \pm SEM of 3 independent experiments in duplicates.* $p < 0.05$ compared to control; § $p < 0.05$ compared to control or compared to ZO-2 KD.